

**New medium-low temperature hydrothermal geothermal district
heating system based on distributed electric compression heat pumps
and a centralized absorption heat transformer**

Fangtian Sun^{a,b*}, Baoru Hao^a, Lin Fu^c, Hongwei Wu^d, Yonghua Xie^a, Haifeng Wu^a

^a. Beijing Research Center of Sustainable Energy and Buildings, Beijing University of Civil

Engineering and Architecture, 100044 Beijing, China

^b. Department of Civil Engineering, Technical University of Denmark, 2800 Lyngby, Denmark

^c. Department of Building Science and Technology, Tsinghua University, 100084 Beijing, China

^d. School of Physics, Engineering and Computer Science, University of Hertfordshire, AL10 9AB,

Hatfield, United Kingdom

* Corresponding author. Tel.: +86 010 68322133; fax: +86 010 88361680

E-mail address: sun_fangtian@163.com

ABSTRACT:

Development of geothermal heat for district heating has attracted considerable attention in China. However, transporting geothermal heat for long distance has become the bottleneck for developing large-scale medium-low temperature hydrothermal geothermal fields that located far away from heat load areas. To solve this problem, a new medium-low temperature hydrothermal geothermal district heating system based on distributed electric compression heat pumps and a centralized absorption heat transformer is proposed and evaluated both from the aspects of thermodynamic performance and economic benefit. Analysis of the results may lead to following main conclusions: (i) for the proposed system, its cost-effective main line length of the

primary heating network is about 10 kilometers. (ii) the annual coefficient of performance, annual product exergy efficiency, and heating cost of the proposed system are found to be 24.5, 61.4% and 55.62 ¥/GJ, respectively. The centralized absorption heat transformer can reduce irreversible loss of the heating station and improve performance of distributed electric compression heat pumps. (iii) Unlike the conventional medium-low temperature hydrothermal geothermal district heating system with longer distance of transporting geothermal heat, the annual coefficient of performance and annual product exergy efficiency of the proposed one can be improved by about 4.34 and 7.4%, respectively.

Keywords: Sustainable district heating; Hydrothermal geothermal; Long heat transportation distance; Distributed compression heat pump; Centralized absorption heat transformer; Emission-reduction potential

Nomenclature

GDH-DCHP-CAHT new medium-low temperature hydrothermal geothermal district heating system based on distributed electric compression heat pumps and a central absorption heat transformer	<i>APEE</i>	annual system product exergy efficiency
	<i>AC</i>	amortization cost, ¥/year
	<i>IC</i>	investment capital, ¥
	<i>n</i>	time, year
	<i>i</i>	annual interest rate
GDH-NGFB medium-low temperature hydrothermal geothermal district heating system with a natural gas fired boiler	<i>Sub indexes</i>	
	<i>lw</i>	water in the primary heating network
	<i>whe</i>	water-to-water heat exchanger
PHN primary heating network	<i>out</i>	outlet
SHN secondary heating network	<i>aht</i>	absorption heat transformer
<i>m</i> mass flow rate, kg/s	<i>con</i>	condenser
<i>h</i> specific enthalpy, J/kg	<i>ngb</i>	natural gas fired boiler
<i>T/t</i> temperature, K/°C	<i>lhv</i>	lower heating value
<i>Qh</i> heating capacity, W	<i>gw</i>	geothermal water
<i>B</i> natural gas consumption rate, kg/s	<i>in</i>	inlet
<i>N</i> power, W	<i>o</i>	outdoor air temperature
η efficiency	<i>abs</i>	absorber
<i>R</i> resistance coefficient of pipeline network	<i>eva</i>	evaporator
<i>k</i> absolute roughness of pipe wall, m	<i>gen</i>	generator
ρ density, kg/m ³	<i>cow</i>	cooling water
<i>d</i> diameter, m	<i>r</i>	refrigerant
ΔP pressure drop, Pa	<i>rp</i>	refrigerant pump
ζ local resistance coefficient	<i>chp</i>	compression heat pump
<i>l</i> length of pipeline	<i>2w</i>	water in the secondary heating network
<i>ex</i> specific exergy, J/kg	<i>com</i>	compressor
<i>s</i> specific entropy, J/(kg.K)	<i>l</i>	local resistance
<i>Ex</i> exergy flow, J	<i>J</i>	number
τ time, second	<i>wp</i>	water pump
<i>Q</i> thermal energy, J	<i>cw</i>	circulating water
<i>E</i> electricity consumption, J	<i>dh</i>	district heating
<i>An</i> anergy, J	<i>0</i>	referred temperature
<i>ACOP</i> annual system coefficient of performance		

1. Introduction

Nowadays, in Northern China, about 1.78×10^9 GJ medium-low temperature hydrothermal geothermal energy is available for district heating annually. In addition, space distribution of the hydrothermal geothermal fields is extremely uneven due to complicated geotectonic movements [1-2]. It is recognized that developing a medium-low temperature hydrothermal geothermal sources for district heating can not only contribute to meeting the growing demand of heat load due to the rapid development of China's urbanization, but also benefit for the reduction of the emission of atmospheric pollutants during the heating period [3]. In the majority of the cases, however, many large-scale medium-low temperature hydrothermal geothermal fields are located far away from the heat load areas [4]. Therefore, there is an urgent need to increase cost-effective distance of transporting geothermal heat to maximize the benefits.

For the primary heating network, a smaller temperature difference between supply and return can bring a high initial investment and more electricity consumption of water pumps. Additionally, it can also lead to high running cost and short cost-effective distance of transporting heat. As far as the existing medium-low temperature hydrothermal geothermal district heating systems are concerned, the cost-effective distances of transporting geothermal heat could be shorter when lower supply temperature and smaller temperature difference between supply and return of the primary heating network are applied [5-6]. In general, existing medium-low

temperature hydrothermal geothermal district heating systems are normally developed with medium-low temperature hydrothermal geothermal heat sources close to the heat load areas. It has proved that the existing systems could not be applied efficiently when it is far away from heat load areas [7]. It is indicated that increasing the temperature difference between supply and return of the primary heating network could contribute to the increase of the cost-effective distance of transporting heat [8-9]. Thus, the medium-low temperature hydrothermal geothermal district heating system with bigger temperature difference between supply and return of the primary heating network would be a feasible solution to develop large-scale medium-low temperature hydrothermal geothermal fields located far away from heat load areas.

Concerning the primary heating network, increasing supply temperature or reducing return temperature could help to increase the temperature difference between supply and return. The gas-fired absorption heat pump type I has the potential to upgrade the geothermal heat in order to achieve higher temperature in the heating station. However, this technology has its own limitations since it would consume a certain amount of natural gas and discharge a large amount of atmospheric pollutants [10-11]. The medium-high temperature electric compression heat pump could be another option to upgrade the medium-low temperature geothermal heat to achieve higher temperature in the heating station [12], but its coefficient of performance (COP) would become lower due to higher heating temperature [13-14]. Moreover, constructing power or natural gas transmission infrastructure over a long distance would lead to high

initial investment and high running cost. As a consequence, both the above mentioned technologies are not realistic when the large scale medium-low temperature hydrothermal geothermal fields are located far away from heat load areas.

Absorption heat transformer is the absorption heat pump type II, and its working principle is significantly different from that of the absorption heat pump type I [15].

Fig. 1 (a) and (b) illustrate respectively the two types of cycle (type I and II) of a single-effect absorption heat pump.

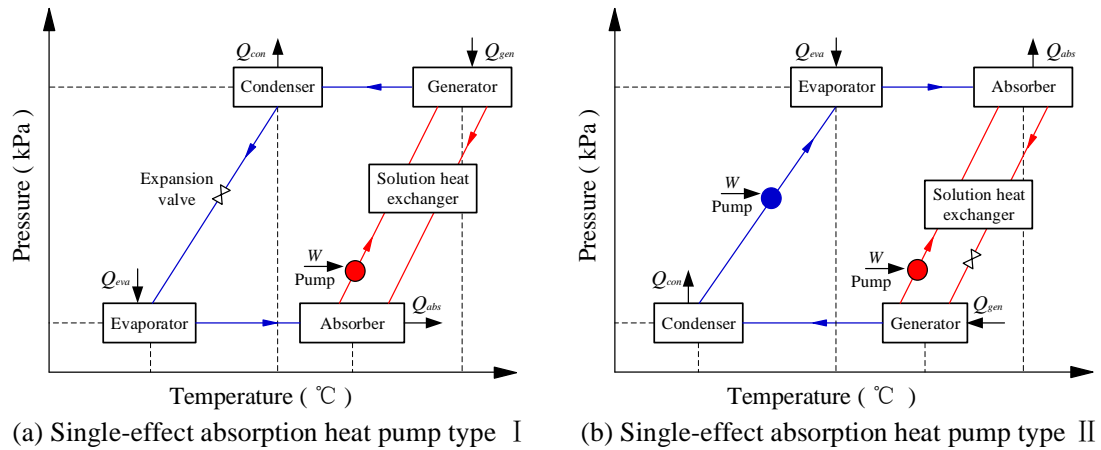


Fig. 1. Cycle schematics of single-effect absorption heat pump type I and II

The absorption heat pump type I driven by high-temperature heat is normally used to upgrade the low-temperature heat to reach medium-temperature. While the absorption heat transformer driven by medium-temperature heat is generally used to upgrade part of the medium-temperature heat to achieve high temperature. Obviously, the absorption heat transformer can be used to upgrade medium-low temperature hydrothermal geothermal heat to obtain higher temperature, but it needs lower temperature heat carrier to take part of the low-temperature heat, which is converted

from medium-low temperature geothermal heat in condenser [16-17]. Therefore, lower return temperature of the primary heating network can help to utilize more hydrothermal geothermal heat by applying the absorption heat transformer, and increase the supply temperature of the primary heating network without consuming any fossil fuel.

Reducing return temperature of the primary heating network contributes to increasing temperature difference between supply and return for longer cost-effective distance of transporting heat [18-19]. Both the absorption heat exchanger [20] and the ejector heat exchanger [21] can be used to reduce the return temperature of the primary heating network in the heating substation, but they need to be driven by supply water of the primary heating network at a temperature ranging from 120 °C to 150 °C. For the medium-low temperature hydrothermal geothermal district heating systems, higher supply temperature of the primary heating network is generally achieved by using the gas fired absorption heat pumps type I and the gas fired boilers [22], and it would result in greater consumption of natural gas and large amount of emission of atmospheric pollutants. Thus, the absorption heat exchanger or the ejector heat exchanger is not a better choice for the medium-low temperature hydrothermal geothermal district heating systems with long distance of transporting geothermal heat. The electric compression heat pump distributed in the heating substation can be used to reduce the return temperature of the primary heating network, and in comparison to the absorption heat exchanger and the ejector heat exchanger, it does not require higher supply temperature

of the primary heating network [23]. Besides, the electric compression heat pumps distributed in the heating substations help to utilize existing power transmission infrastructure in urban districts, and they would consume a certain amount of electricity during the heating period. For the district heating system based on distributed electric compression heat pumps, larger capacity of heating results in greater demand of electricity.

In Northern China, it is recognized that the district heating system based on the combined heat and power system is the main heating mode due to higher thermal efficiency. The combined heat and power system is normally controlled by the thermal led strategy, and thus larger capacity of heating would lead to larger capacity of electricity generation. However, there always exists mismatch between demand for heat and demand for electricity [24-25]. During the heating period, it is noted that the generation of electricity generally exceeds the demand of electricity in Northern China, and thus operational flexibility of the combined heat and power systems is restricted to a large extent [26-27]. For the medium-low temperature hydrothermal geothermal district heating systems, introducing the electric compression heat pumps into the heating substations not only contributes to reducing return temperature of the primary heating network, but also helps to improve operational flexibility of the combined heat and power systems. From the mechanism research's point of view, the main objective of the present work is to propose a new medium-low temperature hydrothermal geothermal district heating system based on distributed electric compression heat

pumps and a centralized absorption heat transformer (GDH-DCHP-CAHT) which can be applied to develop the large-scale medium-low temperature hydrothermal geothermal fields located far away from heat load areas.

2. Description of the proposed district heating system

In the current study, a new GDH-DCHP-CAHT has been developed, as shown in

Fig. 2.

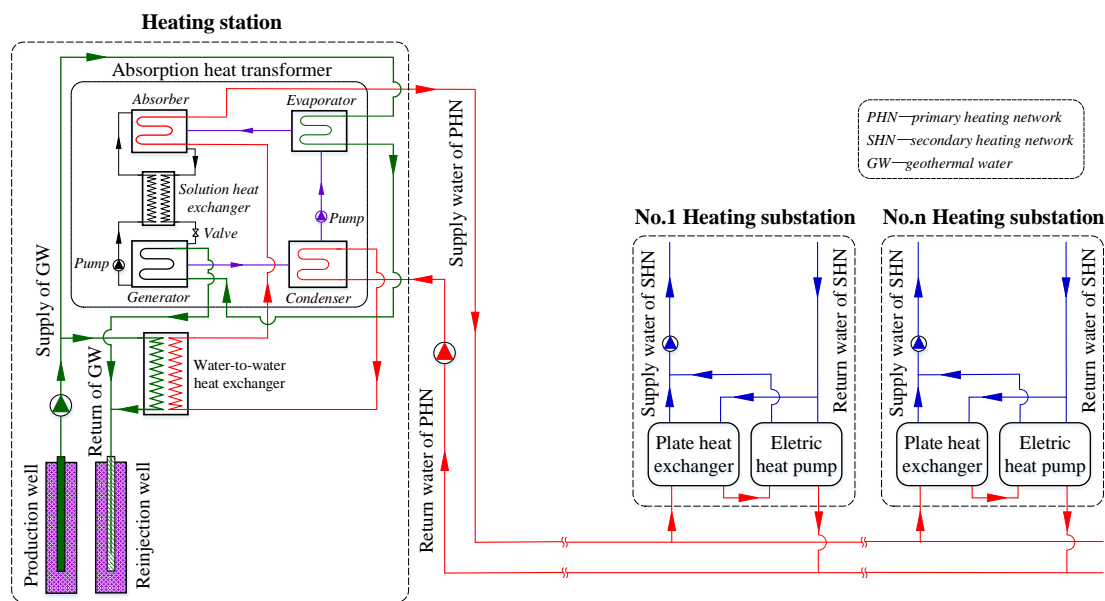


Fig. 2. Schematic diagram of the proposed GDH-DCHP-CAHT

As for the proposed GDH-DCHP-CAHT, an absorption heat transformer working with lithium bromide solution is located in the heating station, and an electric compression heat pump as well as a plate heat exchanger are located in each heating substation. A schematic representation of the electric compression heat pump distributed in the heating substation is illustrated in Fig. 3.

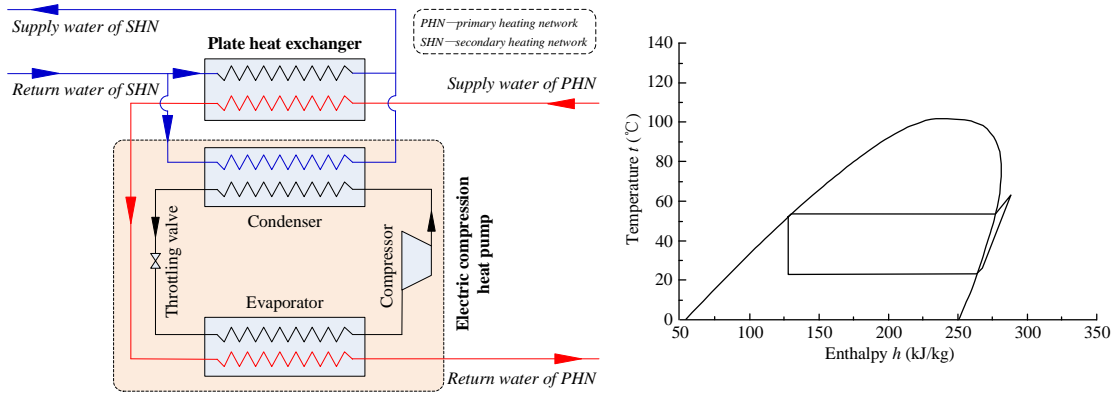


Fig. 3. A schematic representation of the electric compression heat pump distributed in the heating substation

In order to clearly clarify the characteristics of the proposed GDH-DCHP-CAHT, a conventional medium-low temperature hydrothermal geothermal district heating system with a natural gas fired boiler (GDH-NGFB) is introduced, as illustrated in Fig.4.

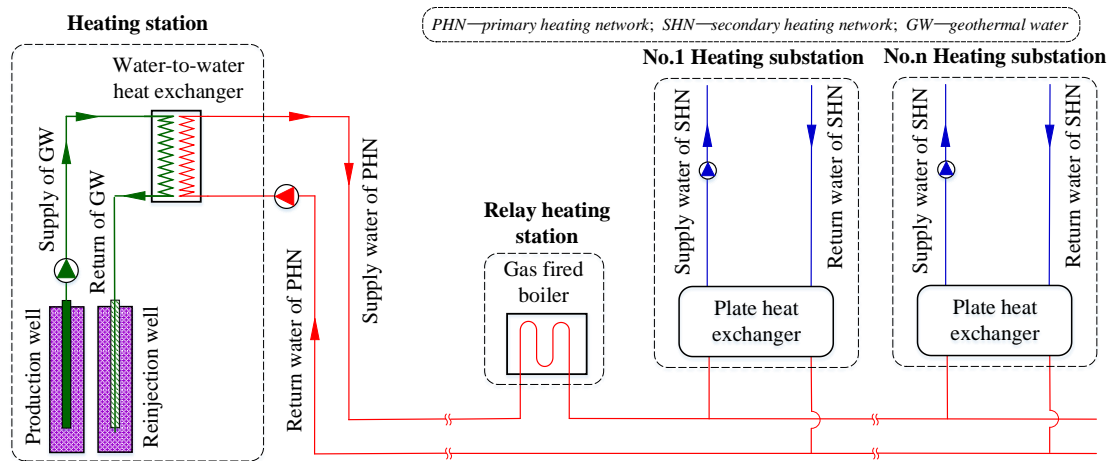


Fig. 4. Overall schematic of the GDH-NGFB

With regard to these two medium-low temperature hydrothermal geothermal district heating systems, both heat users and the secondary heating network are the same, and thus they are not discussed in the following sections.

2.1. Operating principle of the proposed GDH-DCHP-CAHT

(1) Heating station

In the heating station, the geothermal water from the production well is divided into two parts. The first part, used as the heating source, flows into the water-to-water heat exchanger. While the second part, served as the driving heat source, enters into the evaporator and the generator of the absorption heat transformer one by one. Two parts of the cooled geothermal water are merged before reaching the inlet of the reinjection well.

The return water of the primary heating network initially flows into the condenser of the absorption heat transformer where it is heated by the low pressure refrigerant. Afterwards, the heated circulating water in the primary heating network from the condenser flows into the water-to-water heat exchanger, and it is heated by one part of geothermal water. Finally, the heated circulating water from the water-to-water heat exchanger enters into the absorber of the absorption heat transformer, then it is further heated by the higher temperature lithium bromide solution.

For the absorption heat transformer working with lithium bromide solution, water is heated to achieve high pressure steam in the evaporator and subsequently flows into the absorber. In the absorber, the strong lithium-bromide solution absorbs the high pressure steam from the evaporator and the solution becomes weak. The weak lithium-bromide solution is initially cooled by the strong solution from the generator in the solution heat exchanger, and then enters into the low pressure generator. In the generator, the weak lithium-bromide solution gets heat from the hydrothermal geothermal water and it becomes strong lithium-bromide solution and low pressure steam. The low

pressure steam flows into the condenser, and it is cooled to water by the lower temperature return water of the primary heating network. Finally, the low pressure water from the condenser is pumped to the high pressure evaporator by a refrigerant pump. The low pressure strong lithium-bromide solution is pumped into the solution heat exchanger by a solution pump, then it is heated by the weak solution. The heated strong lithium-bromide solution flows into the absorber and takes high pressure steam, which is from the evaporator. In this way, the medium-low temperature hydrothermal geothermal heat is transferred from the geothermal water to the circulating water in the primary heating network.

The geothermal heat is initially transferred from geothermal water to the circulating water in the primary heating network by using both the absorption heat transformer and the water-to-water heat exchanger. Afterwards, it is transported and distributed to the heating substations through the primary heating network.

(2) Heating substation

In the heating substation, the return water of the secondary heating network is divided into two parts. One part flows into the plate heat exchanger, then it is heated by the circulating water in the primary heating network. The other part enters into the condenser of the electric compression heat pump, at which it is heated by the high-temperature refrigerant. Finally, the two parts of the heated circulating water in the secondary heating network are merged at the outlet of the supply water of the secondary heating network.

In the current study, the supply water of the primary heating network, working as the heating source flows into the plate heat exchanger initially. It then enters into the evaporator of the electric compression heat pump serving as the low temperature heat source. As a consequence, the circulating water in the primary heating network is cooled to lower temperature. In the end, the lower temperature circulating water in the primary heating network is served as the return water, and flows back to the heating station through the primary heating network.

With regard to the electric compression heat pump, the refrigerant is initially heated to gaseous refrigerant by the circulating water in the primary heating network in the evaporator. Then it is compressed to a condensing pressure by the compressor. In the condenser, the high-pressure gaseous refrigerant is cooled to liquid by part of the circulating water in the secondary heating network. After that, the liquid refrigerant passes by a throttling valve and its pressure is reduced to the evaporating pressure. Finally, the low pressure gas-liquid mixture refrigerant is heated in the evaporator by the circulating water in the primary heating network. It is necessary to note that, one part of the hydrothermal geothermal heat is transferred to the circulating water in the secondary heating network.

In the heating substation, the geothermal heat is transferred from the circulating water in the primary heating network to that in the secondary heating network by using both the electric compression heat pump and the plate heat exchanger, and then it is transported to the heat users through the secondary heating network. It needs to

be stressed here that the return temperature of the primary heating network is much lower than that of the secondary heating network, while the supply temperature of the primary heating network is equal to that of the geothermal water. Thus, the temperature difference between supply and return of the primary heating network becomes much bigger for longer cost-effective distance of transporting geothermal heat.

2.2. Features of the proposed GDH-DCHP-CAHT

In the proposed GDH-DCHP-CAHT, the absorption heat transformer that centralized in the heating station will be used to produce higher temperature supply water of the primary heating network. Meanwhile, the electric compression heat pumps distributed in the heating substations will be used to achieve lower temperature return water of the primary heating network. Therefore, the proposed GDH-DCHP-CAHT will have bigger temperature difference between supply and return of the primary heating network without consuming any fossil fuel during the heating period. Moreover, the distributed electric compression heat pumps could help to improve the synchronization between the demand of the heat load and the demand of electricity for the combined heat and power systems in winter.

3. Thermodynamic model and evaluation indicators

3.1. Thermodynamic model

(1) Water-to-water heat exchanger

In the current work, the model for the water-to-water heat exchanger is based on

Ref. [28], and its energy conservation equations can be expressed as follows:

$$m_{1w}[h_{1w,whe,out}(t_o) - h_{1w,aht,con,out}(t_o)] = m_{gw,whe}[h_{gw,in} - h_{gw,whe,out}(t_o)] \quad (1)$$

$$Qh_{whe}(t_o) = m_{1w}[h_{1w,whe,out}(t_o) - h_{1w,aht,con,out}(t_o)] \quad (2)$$

(2) Absorption heat transformer

Ref. [29] is considered to build the model for the absorption heat transformer, and

the energy conservation equations can be obtained by using the following formulas:

$$Qh_{aht,con}(t_o) = m_{1w}[h_{1w,aht,con,out}(t_o) - h_{1w,in}(t_o)] \quad (3)$$

$$Qh_{aht,abs}(t_o) = m_{1w}[h_{1w,aht,out}(t_o) - h_{1w,whe,out}(t_o)] \quad (4)$$

$$Qh_{aht,eva}(t_o) = m_{gw,aht}[h_{gw,in} - h_{gw,aht,eva,out}(t_o)] \quad (5)$$

$$Qh_{aht,gen}(t_o) = m_{gw,aht}[h_{gw,aht,eva,out}(t_o) - h_{gw,aht,out}(t_o)] \quad (6)$$

$$COP_{aht} = \frac{Qh_{aht,abs}(t_o)}{Qh_{aht,eva}(t_o) + Qh_{aht,gen}(t_o)} \quad (7)$$

$$N_{rp}(t_o) = m_{r,aht}[h_{r,rp,out}(t_o) - h_{r,rp,in}(t_o)]/\eta_{rp} \quad (8)$$

(3) Natural gas fired boiler

$$Qh_{ngb}(t_o) = \eta_{ngb} \cdot B \cdot h_{ihv} \quad (9)$$

$$Qh_{ngb}(t_o) = m_{1w}[h_{1w,ngb,out}(t_o) - h_{1w,ngb,in}(t_o)] \quad (10)$$

(4) Electric compression heat pump

The energy conservation equations of the electric compression heat pump can be

written as follows [30-31]:

$$N_{com}(t_o) = m_{r,chp}(t_o)[h_{r,eva,out}(t_o) - h_{r,com,out}(t_o)] \quad (11)$$

$$Qh_{chp,eva}(t_o) = m_{1w,whe}[h_{1w,whe,out}(t_o) - h_{1w,out}(t_o)] \quad (12)$$

$$Qh_{chp,con}(t_o) = m_{2w,chp}[h_{2w,chp,con,out}(t_o) - h_{2w,in}(t_o)] \quad (13)$$

$$COP_{chp} = Qh_{chp,eva}(t_o)/N_{com}(t_o) \quad (14)$$

(5) Primary heating network

$$R = 6.88 \times 10^3 \cdot K^{0.25} \frac{m^2}{\rho \cdot d^{5.25}} \quad (15)$$

$$\Delta P_l = \sum \zeta \frac{\rho \cdot u^2}{2} \quad (16)$$

$$\Delta P = \sum (R_j \cdot l_j + \Delta P_{l,j}) \quad (17)$$

(6) Water pump

Power of water pump is calculated as follows:

$$N_{wp}(t_o) = \frac{m_{cw} \cdot \Delta P}{\rho_{cw} \cdot \eta_{wp}} \quad (18)$$

(7) District heating system

During the heating period, heating load, annual geothermal heat input, annual electricity consumption and annual heat output can be expressed as follows:

$$Qh_{gh}(t_o) = m_{gw}(t_o) \cdot [h_{gw,in}(t_o) - h_{gw,out}(t_o)] \quad (19)$$

$$N_{dh}(t_o) = N_{cwp}(t_o) + N_{rp}(t_o) + N_{com}(t_o) \quad (20)$$

$$Q_{gh} = \int_{t_o=t_1}^{t_o=t_2} Qh_{gh}(t_o) d\tau(t_o) \quad (21)$$

$$E_{dh} = \int_{t_o=t_1}^{t_o=t_2} N_{dh}(t_o) d\tau(t_o) \quad (22)$$

$$Q_{dh} = \int_{t_o=t_1}^{t_o=t_2} [Qh_{gh}(t_o) + N_{dh}(t_o)] d\tau(t_o) \quad (23)$$

3.2. Exergy analysis model

Specific exergy is calculated as follows [32]:

$$ex = (h - h_0) - T_0(s - s_0) \quad (24)$$

The chemical specific exergy is calculated as follows [33]:

$$ex_{y,ch} = \sum y_j e_j^0 + RT_0 \sum y_j \ln y_j \quad (25)$$

Mass conservation equation is expressed as follows:

$$\sum m_{in,j} + \sum m_{out,j} = 0 \quad (26)$$

Energy conservation equation is given as follows:

$$\sum Qh_{in,j} + \sum(m_{in,j} \cdot h_{in,j}) - \sum(m_{out,j} \cdot h_{out,j}) = 0 \quad (27)$$

Exergy conservation equation is given as follows:

$$\sum [Qh_j (1 - T_0/T)] + \sum Ex_{N,j} + \sum(m_{in,j} ex_{in,j}) - \sum m_{out,j} ex_{out,j} = \sum An_j \quad (28)$$

3.3. Evaluation indicators

Both coefficient of performance and product exergy efficiency for the current medium-low temperature hydrothermal geothermal district heating system will vary with the increase of outdoor air temperature. Thus, performance of the medium-low temperature hydrothermal geothermal district heating system should be assessed from the aspect of the whole heating period. For the aim of analysis, annual coefficient of performance (*ACOP*) and annual product exergy efficiency (*APEE*) of the medium-low temperature hydrothermal geothermal district heating system are presented [34].

The annual coefficient of performance of the district heating system is defined as the ratio of annual heat output to annual electricity consumption, and it is expressed as:

$$ACOP = \frac{\int Qh_{dh} d\tau}{\int (N_{wp} + N_{rp} + N_{com}) d\tau} \quad (29)$$

The annual product exergy efficiency of district heating system is defined as the ratio of the annual product exergy output of the secondary heating network to the sum of the annual exergy input of both hydrothermal geothermal water, natural gas and annual electricity consumption, and it is calculated as follows:

$$APEE = \frac{\int m_{2w}(ex_{2w,out} - ex_{2w,in}) d\tau}{\int [m_{gw}(ex_{gw,in} - ex_{gw,out}) + N_{wp} + N_{rp} + N_{com} + m_{ng}(ex_{ng,in} - ex_{ng,out})] d\tau} \quad (30)$$

The annual electricity consumption of district heating system is the sum of annual electricity consumption of water pumps, refrigerant pumps, and compressors.

4. Case study

The case study selected for the proposed medium-low temperature hydrothermal geothermal district heating system is located in Northern China with heating load of 200 MW. Annual heating period is 123 days.

Topology of the primary heating network is exhibited in Fig.5.

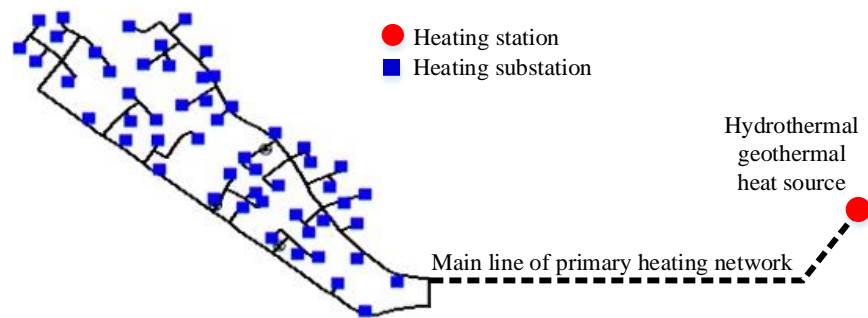


Fig. 5. Topology of the primary heating network

4.1. Design parameters

To analyze the thermodynamic performance and financial benefit of the proposed GDH-DCHP-CAHT and the GDH-NGFB, some information is given as follows:

- (1) Outdoor and indoor design temperatures are $-9.0\text{ }^{\circ}\text{C}$ and $18.0\text{ }^{\circ}\text{C}$ for space heating [35].
- (2) Heat loss of the district heating system accounts for 5.0% of the heating load [36-37].
- (3) For the distributed electric compression heat pump, R134a is selected as the refrigerant, and mechanical efficiency of the compressor and efficiency

of motor are 90% [38-39].

- (4) Thermal efficiency of the natural gas fired boilers is 95% [40].
- (5) According to the current gas-fired power plants, 55% of energy in natural gas can be converted to electricity [41-42].
- (6) The primary heating network and the secondary heating network are two different closed-circuit and their mass flow rates are constant during the heating period.
- (7) The referred temperature and pressure for calculating exergy are $-9.0\text{ }^{\circ}\text{C}$ and $101,325\text{ Pa}$, respectively.
- (8) Prices of electricity and heat are 0.7995 ¥/kWh and 30 ¥/m^2 respectively, and annual interest rate is 4.8%.
- (9) Geothermal heat resource tax is 1 ¥/m^3 according to the requirements of Resource Tax Rates [43-44].

Table 1 listed the main thermal parameters of the proposed GDH-DCHP-CAHT and the GDH-NGFB.

Table 1

Main thermal parameters of the proposed GDH-DCHP-CAHT and the CGDH

Subsystem	Equipment	Items	GDH-DCHP-CAHT	GDH-NGFB
Heating station	Water-to-water heat exchanger	Heating capacity (MW)	152.070	159.630
		Outlet temperature (°C)	70.0	65.0
	Absorption heat transformer	Heating capacity (MW)	39.333	—
		COP (W/W)	0.485	—
		Outlet temperature of condenser (°C)	30.0	—
		Outlet temperature of absorber (°C)	75.0	—
	Natural gas fired boiler	Heating capacity (MW)	—	40.370
		Outlet temperature (°C)	—	70.0
		Supply temperature (°C)	75.0	70.0
	Primary heating network	—	Return temperature (°C)	25.0
Mass flow rate (kg/s)			914.7	1911.6

		Heating capacity (MW)	122.480	200.000
	Plate heat exchanger	Outlet temperature of SHN (°C)	72.0	55.0
Heating substation		Heating capacity (MW)	77.520	—
		Outlet temperature of SHN(°C)	48.2	—
	Electric compression heat pump	Outlet temperature of PHN (°C)	25.0	—
		COP (W/W)	8.016	—
		Supply temperature (°C)	55.0	55.0
Secondary heating network	—	Return temperature (°C)	40.0	40.0
		Mass flow rate (kg/s)	3186.0	3186.0
		Supply temperature (°C)	75.0	75.0
Geothermal water network	—	Return temperature (°C)	45.0	50.0
		Mass flow rate (kg/s)	1524.5	1524.5

In Table 1, it can be seen clearly, compared to the GDH-NGFB, that the proposed GDH-DCHP-CAHT has higher supply temperature of the primary heating network with more utilization of the geothermal heat. Moreover, the proposed GDH-DCHP-CAHT does not consume any natural gas.

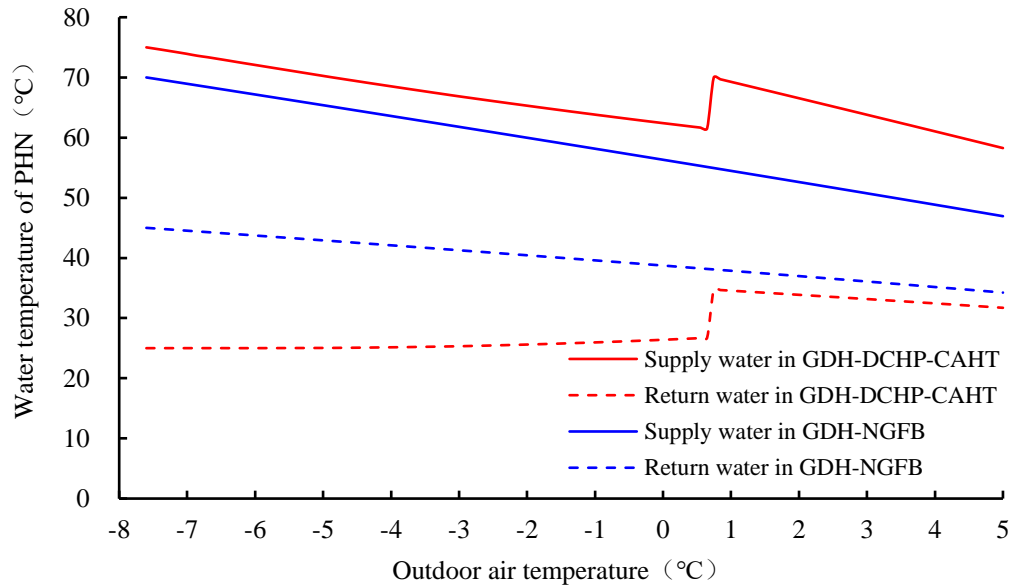


Fig. 6. Temperature curves of the primary heating network during a heating period

From Fig. 6, it is clearly seen that, compared with the GDH-NGFB, the proposed GDH-DCHP-CAHT has bigger temperature difference between supply and return of the primary heating network. In addition, when the outdoor air temperature is lower than 0.7 °C, the supply temperature of the primary heating network decreases with increasing outdoor air temperature. It should be noted that, for the proposed system, the supply and return temperatures of the primary heating network increase suddenly at outdoor air temperature of 0.7 °C. At this case, the electric compression heat pumps distributed in the heating substations will shut down to reduce electricity consumption. And only the plate heat exchangers are used to transfer the geothermal heat from

circulating water in the primary heating network to that in the secondary heating network in the heating substations. To meet the demand of heat load, the supply temperature of the primary heating network needs to be increased for larger heating capacity of the plate heat exchanger. For the case of the outdoor air temperature is higher than 0.7 °C, the supply and return temperatures of the primary heating network start to decrease with the increase of the outdoor air temperature.

4.2. Thermodynamic performance

The main line length of the primary heating network would have an impact on the electricity consumption of the water pumps, and it is expected that both *ACOP* and *APEE* of the district heating system decrease as the main line of the primary heating network becomes longer.

The impacts of the main line length of the primary heating network on *ACOPs* for two hydrothermal geothermal district heating systems are shown in Fig. 7.

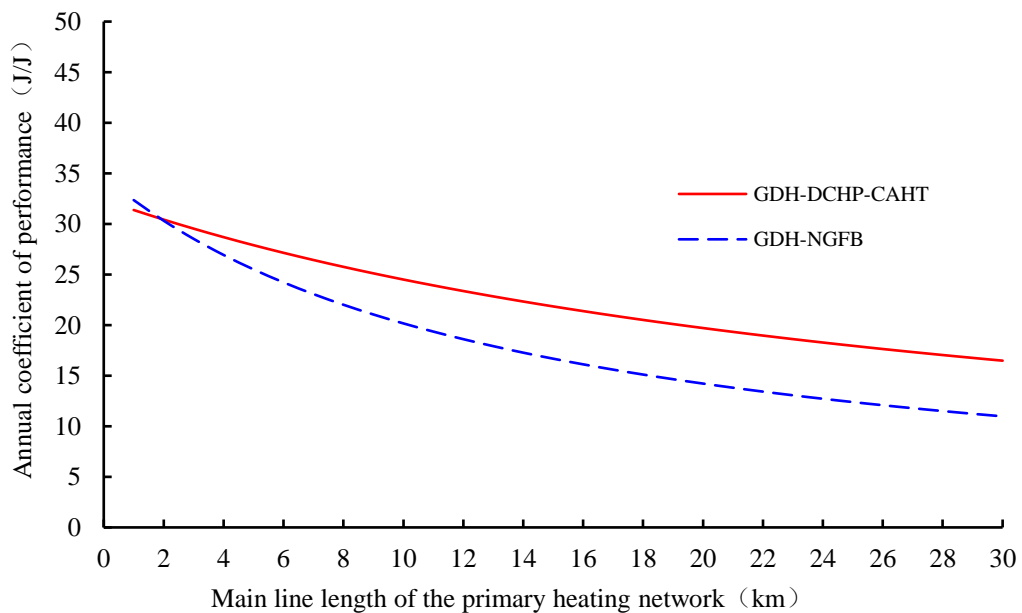


Fig. 7. Relationships between *ACOP* and main line length of the primary heating

network

It can be seen clearly from Fig. 7 that the *ACOPs* for both the proposed GDH-DCHP-CAHT and the GDH-NGFB decrease with the increase of the main line length of the primary heating network. It is noted that when the main line of the primary heating network is shorter than 1.8 kilometers, the *ACOP* of the proposed GDH-DCHP-CAHT is smaller than that of the GDH-NGFB. Whereas when the main line of the primary heating network is longer than 1.8 kilometers, the *ACOP* of the proposed GDH-DCHP-CAHT is larger than that of the GDH-NGFB. It should be also noted that the *ACOP* difference between the proposed GDH-DCHP-CAHT and the GDH-NGFB becomes bigger. This could be explained by the fact that for longer main line of the primary heating network, electricity consumption of the proposed GDH-DCHP-CAHT is much less than that of the GDH-NGFB.

Fig. 8 demonstrates the variation of the *APEE* with the main line length of the primary heating network for the two hydrothermal geothermal district heat systems.

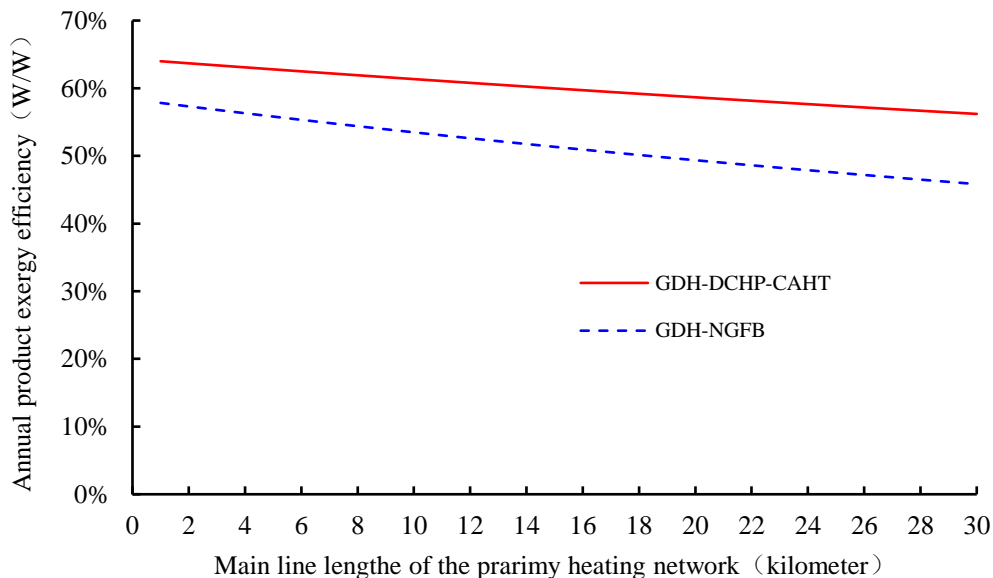


Fig. 8. Variation of *APEE* with the main line length of the primary heating network

From Fig. 8, it can be seen that, the *APEE* for both the proposed GDH-DCHP-CAHT and the GDH-NGFB decrease as the main line of the primary heating network becomes longer. Moreover, the *APEE* of the proposed GDH-DCHP-CAHT is always larger than that of the GDH-NGFB, and the *APEE* difference between the proposed GDH-DCHP-CAHT and the GDH-NGFB becomes bigger with the increase of the main line length of the primary heating network.

From the perspective of thermodynamic performance, the configuration of the proposed GDH-DCHP-CAHT is more advanced than that of the GDH-NGFB when the medium-low temperature hydrothermal geothermal fields are located far away from heat load areas. Therefore, the proposed GDH-DCHP-CAHT is a better choice for the medium-low temperature hydrothermal geothermal district heating systems with longer main line of the primary heating network.

4.3. Potential of energy-saving and emission-reduction

When the main line length of the primary heating network is 10 kilometers, the energy consumption compositions of the two hydrothermal geothermal district heating systems are illustrated in Fig. 9.

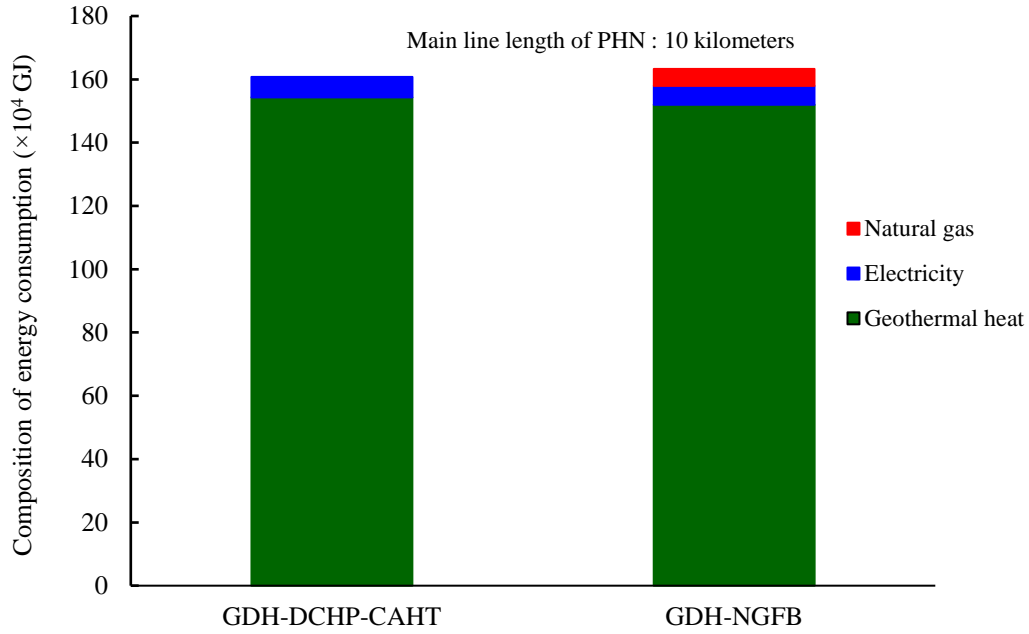


Fig. 9. Energy consumption compositions of two hydrothermal geothermal district heating systems

Fig. 9 shows the total energy consumptions of the two hydrothermal geothermal district heating systems are about 1.61×10^6 GJ during the heating period. The medium-low temperature hydrothermal geothermal heat utilized by the proposed GDH-DCHP-CAHT is about 2.35×10^4 GJ per year more than that by the GDH-NGFB. Besides, the proposed GDH-DCHP-CAHT does not consume any natural gas during the whole heating period. In comparison to the district heating system based on natural gas fired boilers, the proposed GDH-DCHP-CAHT could save natural gas by about 4.438×10^7 Nm³ per year, while the GDH-NGFB could save natural gas by about 3.880×10^7 Nm³ per year. Obviously, energy-saving potential of the proposed GDH-DCHP-CAHT is greater than that of the GDH-NGFB, and thus the proposed GDH-DCHP-CAHT has greater potential of pollutants emission reduction.

Compared with the district heating system based on the natural gas fired boilers, the proposed GDH-DCHP-CAHT could lead to annual emission reduction, i.e. soot emission by about 10.650 tons, SO_x emission by about 0.426 tons, NO_x emission by about 5.725 tons, and CO emission by about 14.203 tons.

From the viewpoints of the energy-saving and emission-reduction, the configuration of the proposed GDH-DCHP-CAHT is more suitable for the medium-low temperature hydrothermal geothermal district heating systems with longer main line of the primary heating network.

Financial benefit is another important factor to consider for assessing feasibility of the medium-low temperature hydrothermal geothermal district heating systems with longer main line of the primary heating network.

4.4. Financial benefit

The investment capital of a district heating system is normally divided into four parts: equipment cost, construction cost, installment cost, and other cost. The equipment costs are normally calculated by the current market average price in China. While the construction cost, installment cost, and other cost are calculated according to the indicators of the current investment estimation in public works in China [45]. The maintenance cost can normally be calculated in terms of 1.5% of the total capital investment of the district heating system. The investment capitals of the two hydrothermal geothermal district heating systems are listed in Table 2.

Table 2. Investment capitals of the two hydrothermal geothermal district heating

systems

Subsystem	Item	GDH-DCHP-CAHT	GDH-NGFB
Heating station	Equipment cost (¥)	410,214,000	409,168,900
	Construction cost (¥)	9,502,800	9,346,100
	Installment cost (¥)	12,670,400	12,461,400
	Other cost (¥)	9,502,800	9,346,100
Primary heating network (10 kilometers)	Equipment cost (¥)	24,933,200	41,082,900
	Construction cost (¥)	26,095,500	33,985,200
	Installment cost (¥)	6,233,300	10,270,800
	Other cost (¥)	19,766,700	15,729,200
Heating substations	Equipment cost (¥)	46,685,000	20,000,000
	Construction cost (¥)	7,002,800	3,000,000
	Installment cost (¥)	9,337,000	4,000,000
	Other cost (¥)	7,002,800	3,000,000
District heating system	Total cost (¥)	588,946,200	571,390,600

Remarks: 1€=7.8063¥ and 1\$=6.5848¥.

From Table 2, it is indicated that the investment capital of the primary heating network subsystem of the proposed GDH-DCHP-CAHT is 24,039,400 ¥ less than that of the GDH-NGFB. However, investment capital of the heating substation subsystem of the proposed GDH-DCHP-CAHT is 40,027,600 ¥ more than that of the GDH-NGFB. As a whole the total investment capital of the GDH-DCHP-CAHT is 17,555,700 ¥ more than that of the GDH-NGFB. It needs to be stressed here that the investment capital of the heating station accounts for about 75% of the total investment capital for the hydrothermal geothermal district heating system.

Heating cost is made up of energy cost and non-energy cost. The energy cost comprises electricity cost, natural gas cost and geothermal heat cost. The non-energy cost consists of labor cost, maintenance cost and amortization cost of investment capital.

Amortization cost (AC) of investment capital (IC) is calculated over the life cycle of the equipment as follows:

$$AC = IC \frac{i(1+i)^n}{(1+i)^n - 1} \quad (31)$$

where, n is taken as 40 for the heating network, whereas $n=15$ for the other equipment.

When the main line length of the primary heating network is 10 kilometers, heating cost compositions of the two hydrothermal geothermal district heating systems are exhibited in Fig. 10.

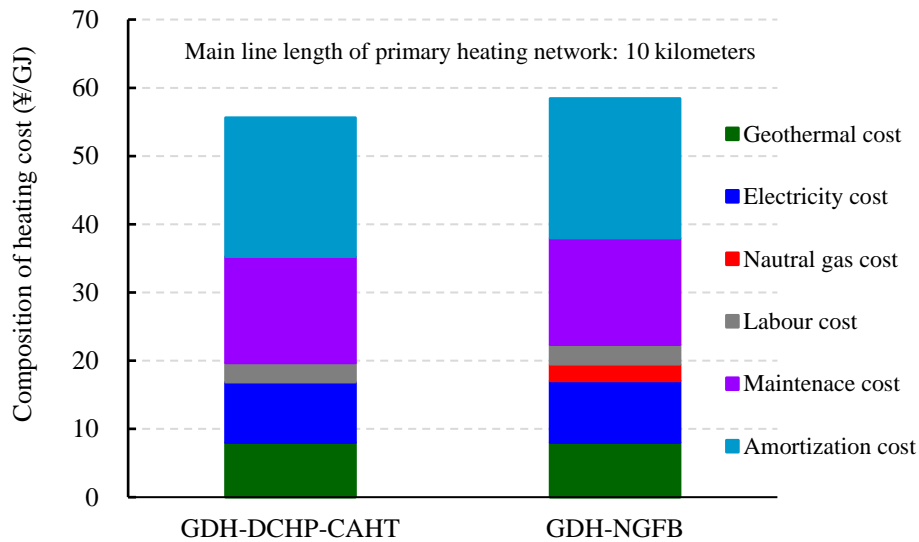


Fig. 10. Heating cost compositions of two hydrothermal geothermal district heating systems

Fig. 10 depicts that the heating cost of the proposed GDH-DCHP-CAHT is 2.82 ¥/GJ lower than that of the GDH-NGFB. The non-energy cost accounts for about 70%

of the heating cost for the proposed GDH-DCHP-CAHT and 67% for the GDH-NGFB. It needs to be pointed out here, that the amortization cost of the investment capital is about 52.5% of the non-energy cost for both hydrothermal geothermal district heating systems. It can be concluded that the bigger initial investment of the hydrothermal geothermal district heating system could have a greater impact on the heating cost and payback period.

It is known that longer main line of the primary heating network leads to the increase of the investment capital of the primary heating network and electricity consumption of water pumps, and thus it would affect the payback period of the hydrothermal geothermal district heating system.

Relationships between payback period and main line length of the primary heating network are shown in Fig. 11.

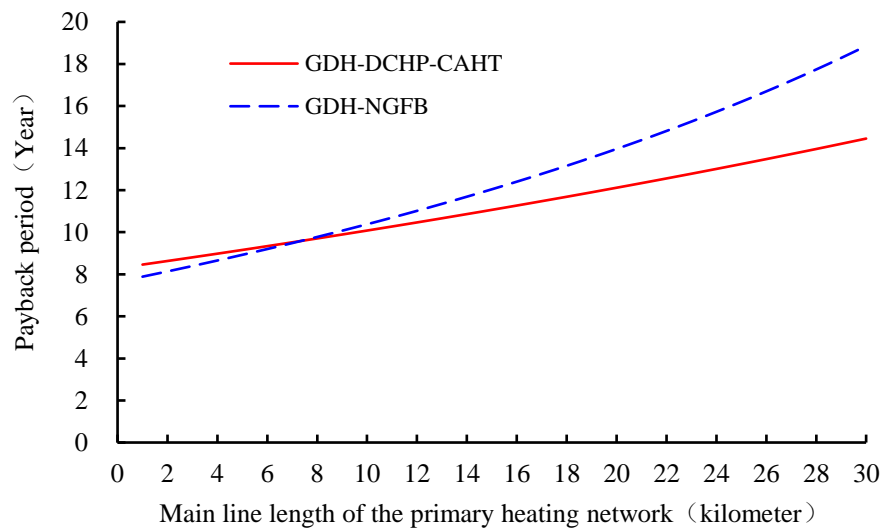


Fig. 11. Relationships between payback period and main line length of the primary heating network

It can be found from Fig. 11, for the two hydrothermal geothermal district heating

systems, that the payback period increases as the main line of the primary heating network becomes longer. It is important to note that when the main line of the primary heating network is longer than 7.2 kilometers, the payback period of the proposed GDH-DCHP-CAHT is shorter than that of the GDH-NGFB. Assume the benchmark of the payback period is 10 years, the cost-effective main line length of the primary heating network would be about 10 kilometers for the proposed GDH-DCHP-CAHT, whereas about 8 kilometers for the GDH-NGFB.

From the aspect of the financial benefit, the proposed GDH-DCHP-CAHT is more suitable for the medium-low temperature hydrothermal geothermal district heating systems with longer main line of the primary heating network, and the GDH-NGFB prefers to one with shorter main line of the primary heating network.

5. Conclusions

The proposed medium-low temperature hydrothermal geothermal district heating system based on distributed electric compression heat pumps and a centralized absorption heat transformer is analyzed from the perspective of thermodynamic performance and economic benefit. Several conclusions could be summarized as follows:

(1) In comparison to the GDH-NGFB, the proposed GHD-DCHP-CAHT has higher thermodynamic performance and greater potential of energy-saving and emission-reduction. When the main line length of the primary heating network is 10 kilometers, annual coefficient of performance and annual product exergy efficiency of

the proposed GDH-DCHP-CAHT are about 24.5 and 61.4%, whereas are 20.2 and 53.9% for the GDH-NGFB. Thus, energy conversion and transfer process of the proposed GDH-DCHP-CAHT is more advanced than that of the GDH-NGFB.

(2) The distributed electric compression heat pumps in the heating substations are mainly used to reduce the return temperature of the primary heating network for achieving bigger temperature difference between supply and return. Lower return temperature of the primary heating network can help to improve the performance of the centralized absorption heat transformer in the heating station.

(3) The centralized absorption heat transformer in the heating station is used to recover available energy of geothermal water for decreasing the irreversible loss of the hydrothermal geothermal energy conversion and transfer process, and contributes to increasing the supply temperature of the primary heating network for obtaining bigger temperature difference between supply and return. Moreover, higher supply temperature of the primary heating network can contribute to performance improvement of the distributed electric compression heat pumps in the heating substations.

(4) Compared with the GDH-NGFB, the proposed GDH-DCHP-CAHT has the advantages such as lower return temperature of the primary heating network and bigger temperature difference between supply and return of the primary heating network, as well as its cost-effective main line length of the primary heating network is increased to about 10 kilometers when the benchmark of the payback period is 10 years.

(5) For the proposed GDH-DCHP-CAHT, the demand for electricity is proportional to the heating capacity, and thus the application of the proposed GDH-DCHP-CAHT could help to improve the operational flexibility of the combined heat and power systems in Northern China.

(6) From the perspective of thermodynamic performance and financial benefit, the configuration of the proposed GDH-DCHP-CAHT is optimal, and it would be a better choice for developing the medium-low temperature hydrothermal geothermal fields located far away from the heat load areas in Northern China.

Acknowledgements

The authors would like to acknowledge the financial support from Science and Technology Support Plan of Beijing Education Committee (KM201810016007). The financial support from the China Scholarship Council (201909960004) is also acknowledged for the support of visiting Technical University of Denmark.

References:

- [1] Wang Gui-ling, Zhang Wei, Liang Ji-yun, Lin Wen-jing, Liu Zhi-ming, Wang Wan-li. Evaluation of Geothermal Resources Potential in China. *Acta Geoscientica Sinica* 2017; 38(4):449-459 (in Chinese).
- [2] J.W. Tester, T.J. Reber, K.F. Beckers, M.Z. Lukawski. Deep geothermal energy for district heating: lessons learned from the U.S. and beyond. *Advanced District*

Heating and Cooling (DHC) Systems, Oxford, 2016.

- [3] Wen Zheng, Yichi Zhang, Jianjun Xia, Yi Jiang. Cleaner heating in Northern China: potentials and regional balances. *Resour. Conserv. Recy.* 2020, 160:104897.
- [4] Jinghui Bai, Weijian Jia, Lixin Liu. Research on the application and development potential of middle-deep geothermal heating technology in Beijing heating market. *J. Heat Vent. Air Cond.* 2017; 47:43-47 (in Chinese).
- [5] Jialing Zhu, Kaiyong Hu, Xinli Lu, Xiaoxue Huang, Ketao Liu, Xiujie Wu. A review of geothermal energy resources, development, and applications in China: Current status and prospects. *Energy* 2015; 93: 466-483.
- [6] Jiewen Deng, Shi He, Qingpeng Wei, Jianfeng Li, Hua Liu, Zhiping Zhang, Hui Zhang. Field test and optimization of heat pumps and water distribution systems in medium-depth geothermal heat pump systems. *Energ. Buildings* 2020, 209:10972.
- [7] Zhang Qi, Chen Siyuan, Tan Zhizhou, Zhang Tiantian, Mclellan Benjamin. Investment strategy of hydrothermal geothermal heating in China under policy, technology and geology uncertainties. *J. Clean Prod.* 2019; 207:17-29.
- [8] Hao Fang, Jianjun Xia, Yi Jiang. Key issues and solutions in a district heating system using low-grade industrial waste heat. *Energy* 2015; 86:589-602.
- [9] Fangtian Sun, Jinzi Zhao, Lin Fu, Jian Sun, Shigang Zhang. New district heating system based on natural gas-fired boilers with absorption heat exchangers. *Energy* 2017; 138: 405-418.
- [10] Ding Lu, Yin Bai, Xueqiang Dong, Yanxing Zhao, Hao Guo, Maoqiong Gong.

- Gas-fired absorption heat pump applied for high-temperature water heating: parametric study and economic analysis. *Int. J. Refrig.* 2020; 119:152-164.
- [11] Fangtian Sun, Lijiao Cheng, Haoyuan Yang, Xinyu Zhao. Energy efficiency analysis of deep geothermal heat supply system based on direct fired absorption heat pump. *J. Heat Vent. Air Cond.* 2017; 47:162-164 (in Chinese).
- [12] Christopher R. Galantino, Steve Beyers, C. Lindsay Anderson, Jefferson W. Tester. Optimizing Cornell's future geothermal district heating performance through systems engineering and simulation. *Energ. Buildings* 2021; 230:110529.
- [13] Baomin Dai, Xiao Liu, Shengchun Liu, Yingying Zhang, Dan Zhong, Yining Feng, Victor Nian, Ying Hao. Dual-pressure condensation high temperature heat pump system for waste heat recovery: Energetic and exergetic assessment. *Energy Convers. And Manag.* 2020; 218:112997.
- [14] Huiming Zou, Xuan Li, Mingsheng Tang, Jiang Wu, Changqing Tian, Dariusz Butrymowicz, Yongde Ma, Jin Wang. Temperature stage matching and experimental investigation of high-temperature cascade heat pump with vapor injection. *Energy* 2020;118734.
- [15] Keith E. Herold, Reinhard Radermacher, Sanford A. Klein. Absorption chillers and heat pumps (Second Edition). CRC press, Taylor & Francis Group, Boca Raton London New York, USA, 2016.
- [16] Falk Cudok, Niccol' o Giannetti, Jos' e L. Corrales Ciganda, Jun Aoyama, P. Babu, Alberto Coronas, Tatsuo Fujii, Naoyuki Inoue, Kiyoshi Saito, Seiichi Yamaguchi,

- Felix Ziegler. Absorption heat transformer - state-of-the-art of industrial applications. *Renew. Sust. Energ. Rev.* 2021; 141:110757.
- [17] M. Hatef Seyyedvalilu, V. Zare, F. Mohammadkhani. Comparative thermoeconomic analysis of trigeneration systems based on absorption heat transformers for utilizing low-temperature geothermal energy. *Energy* 2021;224: 120175.
- [18] Xiaoyun Xie, Yi Jiang. Absorption heat exchangers for long-distance heat transportation. *Energy* 2017; 141: 2242-2250.
- [19] Fangtian Sun, Junlong Li, Lin Fu, Yonghong Li, Ruixiang Wang, Shigang Zhang. New configurations of district heating and cooling system based on absorption and compression chillers driven by waste heat of flue gas from coke ovens. *Energy* 2020; 193: 116707.
- [20] Jian Sun, Lin Fu, Shigang Zhang. Experimental study of heat exchanger basing on absorption cycle for CHP system. *Appl. Therm. Eng.* 2016;102:1280-1286.
- [21] Fangtian Sun, Xu Chen, Lin Fu, Shigang Zhang. Configuration Optimization of an Enhanced Ejector Heat Exchanger Based on an Ejector Refrigerator and a Plate Heat Exchanger. *Energy* 2018; 164: 408-417.
- [22] Fangtian Sun, Xinyu Zhao, Xu Chen, Lin Fu, Lanbin Liu. New configurations of district heating system based on natural gas and deep geothermal energy for higher energy efficiency in northern China. *Appl. Therm. Eng.* 2019; 151: 439-450.
- [23] Fangtian Sun, Yonghua Xie, Svend Svendsen, Lin Fu. New low-temperature

- central heating system integrated with industrial exhausted heat using distributed electric compression heat pumps for higher energy efficiency. *Energies* 2020; 13: 6582.
- [24] Wei Wang, Sitong Jing, Yang Sun, Jizhen Liu, Yuguang Niu, Deliang Zeng, Can Cui. Combined heat and power control considering thermal inertia of district heating network for flexible electric power regulation. *Energy* 2019; 169: 988-999.
- [25] Dacheng Li, Songshan Guo, Wei He, Marcus King, Jihong Wang. Combined capacity and operation optimisation of lithium-ion battery energy storage working with a combined heat and power system. *Renew. Sust. Energ. Rev.* 2021; 140:110731.
- [26] Jiang Lin, Fredrich Kahrl, Xu Lin. A regional analysis of excess capacity in China's power systems. *Resour Conserv Recy* 2018; 129: 93-101.
- [27] Yuwei Chen, Qinglai Guo, Hongbin Sun, Zhengshuo Li, Zhaoguang Pan, Wenchuan Wu. A water mass method and its application to integrated heat and electricity dispatch considering thermal inertias. *Energy* 2019; 181:840-852.
- [28] M.W. Browne, P.K. Bansal. An elemental NTU- ϵ model for vapour-compression liquid chillers. *Int. J. Refrig.* 2001; 24:612-627.
- [29] Yang Jing, Feng Liu, Jun Sui, Taixiu Liu. A novel method and operation strategy for the improved performance of an absorption heat transformer. *Appl. Therm. Eng.* 2020; 178:115548.
- [30] Jinghui Liu, Qinggang Li, Fazhong Wang, Lei Zhou. A new model of screw

- compressor for refrigeration system simulation. *Int. J. Refrig.* 2012; 35:861-870.
- [31] F.W. Yu, K.T. Chan. Improved energy performance of air cooled centrifugal chillers with variable chilled water flow. *Energy Convers. And Manag.* 2008; 49:1595–1611.
- [32] Yunus A. Çengel, Michael A. Boles. *Thermodynamics: An Engineering Approach* (8th edition). McGraw-Hill Education Publisher, Boston, 2015.
- [33] Weicheng Wang, Runtian Ma. *Energy Efficient Utilization of Technology*. Chemical Industry Press, Beijing, 1984 (in Chinese).
- [34] Hrvoje Dorotić, Tomislav Pukšec, Neven Duić. Multi-objective optimization of district heating and cooling systems for a one-year time horizon. *Energy* 2019; 169:319-328.
- [35] Ministry of Housing and Urban-Rural Development of the People’s Republic of China, Design code for heating ventilation and air conditioning of civil buildings (GB 50736-2012), China Architecture & Building Press, Beijing, 2012 (in Chinese).
- [36] Ministry of Housing and Urban-Rural Development of the People’s Republic of China (MOHURD), Industry standard of the People’s Republic of China: Design code for city heating network (CJJ 34-2010), China’s Architecture and Building Press, Beijing, July 2010 (in Chinese).
- [37] Building Energy Research Center of Tsinghua University. Annual report of China building energy conservation 2016, Architecture and Building Press, Beijing, China 2016 (in Chinese).

- [38] J.U. Ahamed, R. Saidur, H.H. Masjuki. A review on exergy analysis of vapor compression refrigeration system. *Renew. Sust. Energ. Rev.* 2011; 15: 1593-1600.
- [39] Yafen Tian, Hao Yuan, Chuang Wang, Huagen Wu, Ziwen Xing. Numerical investigation on mass and heat transfer in an ammonia oil-free twin-screw compressor with liquid injection. *Int. J. Therm. Sci.* 2017; 120: 175-184.
- [40] Defu Che, Yanhua Liu, Chunyang Gao. Evaluation of retrofitting a conventional natural gas fired boiler into a condensing boiler. *Energy Convers. And Manag.* 2004; 45:3251-3266.
- [41] José Eduardo Prata, José Roberto Simões-Moreira. Water recovery potential from flue gases from natural gas and coal-fired thermal power plants: A Brazilian case study. *Energy* 2019; 186:115780.
- [42] Building Energy Research Center of Tsinghua University. Annual report of China building energy conservation 2019, Architecture and Building Press, Beijing, China 2019 (in Chinese).
- [43] Standing Committee of the Beijing Municipal People's Congress on the Specific. Specific Applicable Tax Rates of Beijing Resource Tax and Other Matters. http://www.beijing.gov.cn/zhengce/zhengcefagui/202007/t20200731_1966827.html (in Chinese).
- [44] Standing Committee of the Tianjin Municipal People's Congress on the Specific. Specific Applicable Tax Rates of Beijing Resource Tax and Other Matters.

<http://www.tjrd.gov.cn/flfg/system/2020/07/30/030017384.shtml> (in Chinese).

[45] Standard fixed institute of MOHURD. Indicators of investment in public works estimates. China's Planning Press, Beijing, China, 2007 (in Chinese).